Semiconductor Physics, Quantum Electronics & Optoelectronics, 2014. V. 17, N 4. P. 374-379.

PACS 78.55.Et, 78.67.Bf

Luminescent properties of fine-dispersed ZnS:Cu prepared using self-propagating high-temperature synthesis

Yu.Yu. Bacherikov[1,*], S.E. Zelensky[2], A.G. Zhuk[1], N.A. Semenenko[1], O.S. Krylova[2]
[1]*V. Lashkaryov Institute of Semiconductor Physics, NAS of Ukraine*
*41, prospect Nauky, 03028 Kyiv, Ukraine, *e-mail: Yuyu@isp.kiev.ua*
[2]*Taras Shevchenko Kyiv National University,*
64/13, Volodymyrska str., 01601 Kyiv, Ukraine

Abstract. Fine-dispersed ZnS doped with Cu was prepared using self-propagating high-temperature synthesis. In the photoluminescence excitation spectra, the blue shift of the host lattice excitation peak is observed for powder ZnS:Cu that contains nano- and meso-sized (submicron) particles. The obtained spectra indicate that radiative recombination in meso-sized particles is significantly reduced as compared to micro-sized particles, which can be caused by the increase of non-radiative relaxation processes in surface states.

Keywords: luminescent properties, nanoparticle, radiative recombination.

Manuscript received 27.01.14; revised version received 30.07.14; accepted for publication 29.10.14; published online 10.11.14.

1. Introduction

At the present stage of development of electronics, optoelectronics and computer technologies, many efforts are made in searching new materials for functional elements of integrated circuits, storage media, photovoltaic cells, light-emitting elements, *etc*. Among newly developed materials, a special place is occupied by those containing nanoscale particles of metals and semiconductors, including oxides, sulfides, *etc*. Due to their specific electronic structure, materials based on quantum dots are promising candidates for numerous applications. However, despite the significant amount of currently existing experimental and theoretical works concerning quantum dots, we are still far from complete understanding of physical mechanisms of electron interactions in real nanoparticles and nanomaterials. This problem is also actual for a kind of fine-dispersed materials in which the particle size is intermediate between bulk material and quantum dots, i.e. those materials in which the quantum-sized effects are not fully developed.

Among semiconductor luminophors that have been practically applied, ZnS has a special place. The industrial use of activated ZnS for over 70 years stimulated more profound study of its physical characteristics defining a variety of luminescent properties of this material [1-7]. Nowadays, properties of luminescent centers formed by copper [4-9] and other impurities [10-13] in ZnS have been studied so well that the behavior of impurity atoms in these crystals can be reliably monitored by fluorescent techniques.

Among a variety of methods for synthesis of ZnS, including ZnS nanoparticles, a significant interest is attracted to single-stage synthesis methods. In particular, the method of self-propagating high-temperature synthesis (SHS) is actively developed as a promising one for production of ZnS-based luminophor materials [14, 15]. The replace of traditional oven-based technologies by SHS significantly changes the approaches to preparation of solid materials with predetermined luminescent properties, including the processes of synthesis and subsequent treatment. Technological capabilities of SHS are relatively broad, because SHS allows to grow single

crystals and powders, including nanoscale materials, with "popular" sizes of about 1…5 nm, with doping performed during the synthesis.

The aim of this work was to test the possibilities of self-propagating high-temperature synthesis techniques for production of fine-dispersed ZnS:Cu luminophors with a different content of micro-, meso- and nano-sized particles, and to study their luminescent properties.

2. Experimental procedure and characterization of samples

In this work, for the synthesis of ZnS:Cu by using the SHS method the ingredients Zn and S were taken in stoichiometric ratio, and the concentration of Cu in the mixture was about 1 wt.%. The batch materials were of analytical grade qualifications. The fine-dispersed materials of interest were collected in the traps installed inside the SHS-reactor at different distances from the reaction zone. By choosing geometry of the reactor and positions of the traps, powder materials with a variable content of micro- and nano-sized particles were obtained. As a sample with prevailing micro-sized particles, the powder ZnS:Cu from the reaction zone was used.

The photoluminescence (PL) and photo-luminescence excitation (PLE) spectra were recorded at room temperature using an SDL-2 spectrometer. For PLE spectra, excitation was performed with the use of a DKSSh-150 xenon lamp and MDR-12 monochromator. For PL spectra, an LGI-21 nitrogen laser (λ = 337 nm) was employed, working with the repetition rate of 100 pulses per second. Since this work is focused on comparison of luminescent properties of the same material obtained under different synthesis conditions, the PL spectra were not corrected for spectral sensitivity of the used equipment.

Electron microscopic studies were performed on a Mira 3 LMH FE Scanning Electron Microscope (Schottky field emission gun, FESEM) Tescan. To obtain images of surfaces of the conductive samples, a scanning procedure was performed in a vacuum chamber under the residual gases pressure of 10^{-3} Pa. Maximal resolution was about 1 nm. Fig. 1 shows typical SEM images for fine-dispersed materials obtained under different synthesis conditions. As seen from the images, the synthesized particulate materials are mixtures of fractions of particles of different sizes, including nanoparticles and particles of micron and submicron sizes.

3. Results and discussion

Fig. 2 shows the PL spectra of ZnS:Cu, synthesized using the SHS method. Curve *1* in Fig. 2 corresponds to material from the reaction zone, where the micro-sized particles are dominant (see Fig. 1a), and curves *2* and *3* in Fig. 2 correspond to the content of the traps, where the particles of meso- and nano-sized are present in a large quantity (see Fig. 1b).

Every spectrum shown in Fig. 2 consists of a broad band without visible signs of structure in the blue-green spectral region with the peak position at λ_{max} ~500…525 nm, which is typical for ZnS doped with Cu. It is well known [1, 2, 16] that the blue-green PL spectrum of ZnS:Cu has a hidden structure and usually consists of several Cu-related and self-activated bands. The nature of luminescence centers responsible for blue and green emission in ZnS:Cu was extensively studied in [1, 2, 17-22]. The green Cu-related band (λ_{max} ~510…525 nm) is assigned to the luminescence center corresponding to Cu as a substitute for Zn in the ZnS lattice [1, 2, 18]. The center responsible for blue Cu-related band with λ_{max} ~470 nm is attributed to the associates of a kind of a short-distance donor-acceptor pair Cu_i-Cu_{Zn} [1, 2, 21] or a complex comprising Cu_{Zn}-Cu_{Zn} [18-20]. In the blue-green spectral region, there are also bands related to oxygen centers [1, 18, 22] and self-activated bands of ZnS [1, 2, 19, 20].

The main difference between the PL spectra shown in Fig. 2 is in the position of the maxima and in the bandwidth. Whereas the PL spectrum of the material obtained in the reaction zone (Fig. 2, curve *1*) is a symmetrical band with the maximal emission at the wavelength λ_{max} ~520 nm and halfwidth $\Delta\lambda$ ~ 80 nm, the spectra of materials from traps (Fig. 2, curves *2* and *3*)

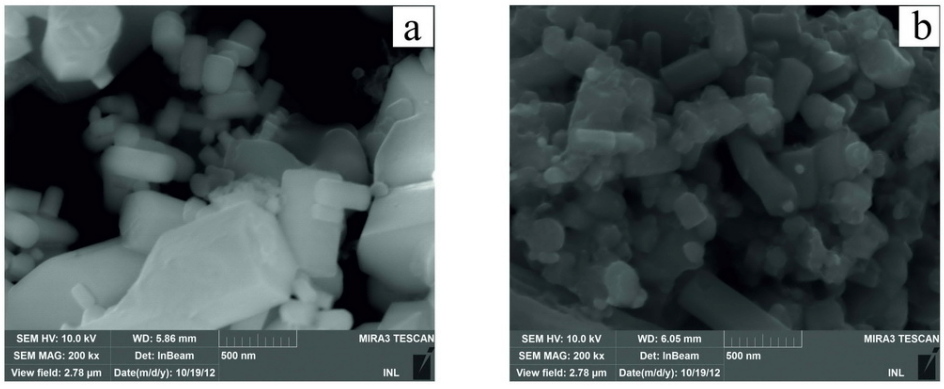

Fig. 1. SEM-images of SHS-synthesized ZnS:Cu powder from the reaction zone (*a*) and from the trap located at the maximal distance from the reaction zone (*b*).

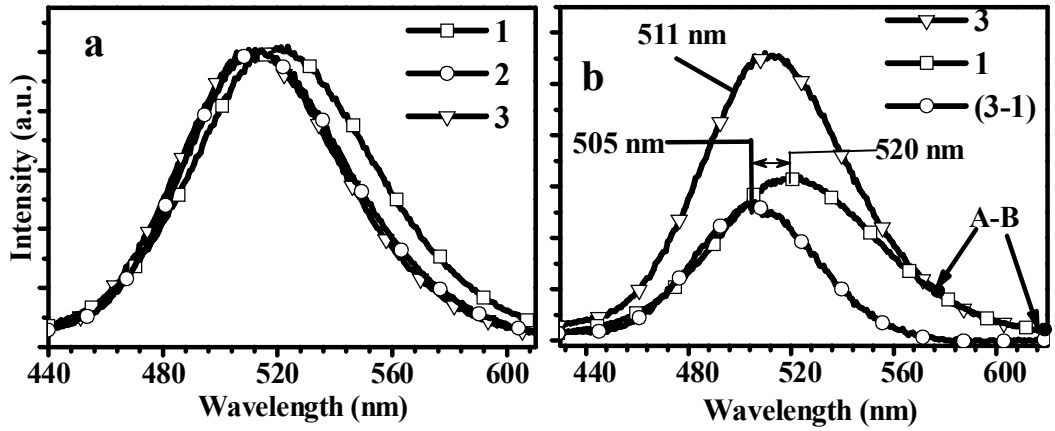

Fig. 2. PL spectra of SHS-synthesized ZnS:Cu. (a) spectra *1–3* are normalized to the maximal intensity, (b) spectra *1* and *3* are linked at the long-wave wings (within the spectral range marked as AB). Curve *1* corresponds to the material from the reaction zone, curves *2* and *3* – to the material from the traps.

have λ_{max} ~510 nm and halfwidth $\Delta\lambda \sim$ 60 nm. According to [8, 9], the position of the maximum in PL spectra of ZnS:Cu depends on the ratio of intensities of blue and green bands, which in turn is determined by the ratio of concentrations of different centers formed by copper [1, 2, 17-22]. During the SHS procedure, thermodynamic conditions of formation of fractions with different particle sizes can be different; hence, localization of Cu in the mentioned fractions can also differ. That is why we suggest that the observed peculiarities of PL spectra of fine-dispersed ZnS:Cu (Fig. 2) can be explained (at least partly) by redistribution of the intensity of blue and green Cu-related bands. However, redistribution of intensities of individual emission bands seems to be not a unique cause of the observed changes of λ_{max} in PL spectra.

According to the SEM data, materials synthesized in the reaction zone and in the traps contain several fractions of particles (micro-, meso-, and nano-sized) with the fraction volume ratio depending on the synthesis conditions. This circumstance provides grounds for approximate extraction of the luminescence corresponding to meso- and nano-fractions from the observed PL spectra. For this purpose, the PL spectrum of the reaction-zone material can be subtracted from the PL spectra of materials from the traps, after preliminary linking the spectra in the long-wave region, as it is shown in Fig. 2, curve (*3-1*). As a result, the positions of maxima of PL of meso- and nano-fractions can be estimated (see Table).

Table. Positions (λ_{max}) and position shifts ($\Delta\lambda$) of PL and PLE spectral components.

Curve	λ_{max}^{PLE}	$\Delta\lambda^{PLE}$	λ_{max}^{PL}	$\Delta\lambda^{PL}$
1	340	–	520	–
2	328	12	506	15
3	325	15	505	14

As it is seen from Table, the position shift of PL bands for meso- and nano-fractions is about 14…15 nm. Such a short-wave shift of PL spectra of fine-dispersed ZnS:Cu fractions as compared to the spectrum of the reaction-zone material (Fig. 2) can be caused by quantum-sized effects in the nanoscale particles, which are present in the trap-collected materials. As it is known [23-29], particulate ZnS with particle sizes $D \le 5…7$ nm clearly shows the quantum-dimensional properties, namely, the PL and interband absorption spectra of these particles are shifted towards shorter wavelengths, and this shift by the order of its magnitude correlates with the observed shift of ~15 nm in the PL spectrum shown in Fig. 2b.

In favour of the above-proposed interpretation of PL spectra of fine-dispersed ZnS:Cu, the following PLE data is presented in Fig. 3. The PLE spectra were recorded for the luminescence spectral intervals of about 1.3 nm surrounding the respective PL maxima: λ_{max} = 520 nm for curve *1* in Fig. 3 and λ_{max} = 510 nm for curves *2* and *3* in Fig. 3. Since the analysis performed is only comparative for different fractions of particulate ZnS:Cu, the spectra given in Fig. 3 are not corrected for non-uniformity of spectral distribution of the radiation source used for excitation and spectral heterogeneity of the monochromator transmission function.

Curve *1* in Fig. 3 corresponds to the reaction-zone material. The figure shows that the spectrum contains the impurity-defect excitation band with λ_{max} = 370 nm, and at shorter wavelengths a curve bend is observed, which can be assigned to interband excitation with a typical for ZnS wavelength of 340 nm [1, 2].

As it is seen from Fig. 3, the PLE spectra of reaction-zone and trap-collected ZnS:Cu have similar structure, including interband and impurity-defect spectral components. It is also seen that the spectra of trap-collected materials are shifted towards shorter wavelengths as compared to the appropriate components of the PLE spectrum of reaction-zone ZnS:Cu. Namely,

for the interband PLE spectral component of the reaction-zone sample with λ_{max} = 340 nm (Fig. 3, curve *1*), the appropriate spectral components of PLE spectra of trap-collected materials are located at λ_{max} = 328 and 325 nm (Fig. 3, curves *2* and *3*). This shift can be attributed to quantum-sized effects in nanoscale fractions. The observed value of shift in the PLE spectra is in good agreement with the above-given estimation of shift in the PL spectra (see Table). We can similarly explain the shift of long-wave bands in PLE spectra presented in Fig. 3. Using the results reported in [26-29], the observed shift of the bands in PLE spectra provides grounds for estimation of the average size of nanoparticles close to 3 nm.

In the spectral characteristics of SHS-produced powdered ZnS:Cu, the following circumstance attracts a particular attention. For the materials collected in traps, the observed PLE spectra (curves *2* and *3* in Fig. 3) do not contain clear visible signs of the presence of the 340 nm band attributed to interband transitions in ZnS, whereas the performed SEM studies of the trap-collected material show the presence of a significant amount of submicron particles. For submicron particles, quantum-sized effects are not relevant, hence the PLE spectra of trap-collected samples were expected to contain the band with λ_{max} ~ 340 nm, at least in the form of the curve

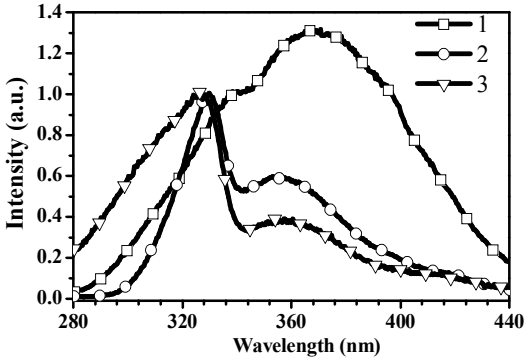

Fig. 3. PLE spectra of SHS-synthesized ZnS:Cu. Numbering of the spectra corresponds to Fig. 2.

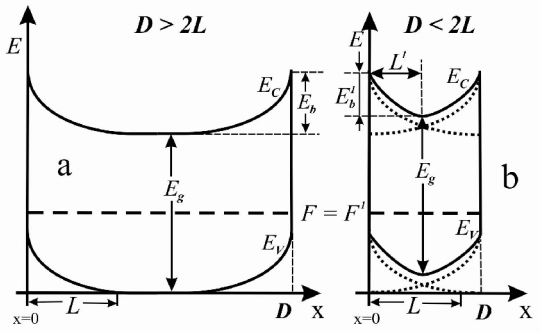

Fig. 4. Energy diagrams for particles with *n*-type conductivity and particle size $D > 2L$ (*a*) and 5…7 nm < $D < 2L$ (*b*).

bend. The mentioned absence of the 340-nm band in the PLE spectra of the trap-collected material indicates that in the meso-sized particles, recombination of carriers produced by band-band absorption is primarily realized non-radiatively. It can be possible if: (i) abovementioned relaxation in the meso-sized particles occurs with easy escape of non-equilibrium carriers out of the recombination zone, (ii) excited radiative centers are located in the depletion zone.

Let us consider possible reasons for the increased role of non-radiative relaxation of photo-excited carriers in the submicron fraction of trap-collected ZnS:Cu. The decrease in the particle size from micron to the submicron one leads to the increase of the influence of surface and near-surface regions on the processes occurring inside the volume. It is plausible to suggest that relaxation via surface states can be one of the main mechanisms of non-radiative relaxation of photo-excited carriers in powder ZnS:Cu [30]. As far as in this work the investigated micro- and meso-particles are produced within the same cycle of synthesis with the same ingredients, we assume that the difference between these particles is their size, whereas the properties of their surfaces can be considered as identical. Consider a space charge region (SCR), which is formed near the crystal surface and impedes diffusion of photo-excited carriers to the surface. Denote the length of SCR as L, and the energy barrier height as E_b. If a particle size D exceeds $2L$, its SCR properties are the same as for bulk crystals. The model pattern of the energy diagram is given in Fig. 4 for the cases $D > 2L$ and 5…7 nm < $D < 2L$. As seen from the figure, in case of 5…7 nm < $D < 2L$, the height and width of the barrier are reduced, which facilitates diffusion of photo-excited carriers to the surface and subsequent non-radiative recombination.

As shown in [31], the length of SCR in high-resistance ZnS crystals is about 100 nm. Foreign inclusions, defects, activators, etc. increase conductivity; hence the length of SCR can also be significantly increased. As follows from the SEM images given in Fig. 1b, in the trap-collected material there are a lot of particles with at least one dimension below the limit of 200 nm. For these particles, the condition $D < 2L$ is satisfied, hence the above-mentioned easy escape of non-equilibrium carriers from the particle volume to its surface can be expected. As it can be seen from Fig. 4, for meso-sized particles, the particle volume becomes a region of strong depletion, where the Fermi level lies closer to the valence band; hence the carrier sticking occurs on the acceptor levels, and radiative recombination becomes depressed.

4. Conclusions

The obtained results indicate that the proposed modified SHS method (trap-equipped SHS) can be used for production of fine-despersed materials based on ZnS:Cu. By using this method, fluorescent powder materials ZnS:Cu can be synthesized with a variable content of

micro-, meso-, and nano-fractions. Observed in the submicron fraction, enhancement of surface non-radiative relaxation of photo-excited carriers opens a possibility for prediction and correction of characteristics of synthesized powder luminophors, as well as for control of the properties of semiconductor structures, for example, for making easier the transport of carriers through the space-charge regions.

Acknowledgements

The authors are grateful for the financial support of Open Company "Technocrat".

References

1. M. Aven and J.S. Prener, *Physics and Chemistry of II–VI Compounds*. N. Y., North-Holland Publ. Company, Amsterdam, 1967.
2. A. Gurevich, *Introduction to the Physical Chemistry of Phosphor Crystals*. Vysshaya Shkola, Moscow, 1971 (in Russian).
3. S. Shionoya // *Intern. Conf. on II-VI Semiconducting Compounds*. New-York, Amsterdam, part 1, 1967.
4. N.A. Vlasenko and A.N. Gergel // *Phys. Status Solidi*, **26**, p. 66-81 (1968).
5. Y.-T. Nien, I.G. Chen, Ch.-Sh. Hwang and Sh.-G. Chu, Copper concentration dependence of structure, morphology and optical properties of ZnS:Cu,Cl phosphor powder // *J. Phys. Chem. Solids*, **69**, p. 366 (2008).
6. A. Suzuki and S. Shionoya // *J. Phys. Soc. Jpn.* **31**, p. 1462 (1971).
7. N.A. Vlasenko and V.S. Khomchenko // *Phys. Status Solidi* (*a*), **19**, p. 137 (1973).
8. Yu. Bacherikov, I. Golovina, and N.V. Kitsyuk, Thermal metamorphosis occurring with ZnS in the process doping from CuCl // *Phys. Solid State*, **48**, p. 1872 (2006).
9. I. Markevich, A. Zhuk, T. Stara, Yu. Bacherikov and N. Korsunska, About the origin of center responsible for Cu-related blue emission band in ZnS:Cu // *J. Lumin.* **145**, p. 71-73 (2014).
10. M. Ollinger, V. Craciun, and R.K. Singh, Nanoencapsulation of ZnS:Ag particulates with indium tin oxide for field emission displays // *Appl. Phys. Lett.* **80**, p. 1927 (2002).
11. G.H. Li, F.H. Su, B.S. Ma, K. Ding, S.J. Xu, and W. Chen, Photoluminescence of doped ZnS nanoparticles under hydrostatic pressure // *Phys. Status Solidi* (*b*), **241**(14), p. 3248-3256 (2004).
12. O.A. Korotchenkov, A. Cantarero, A.P. Shpak, Y.A. Kunitskii, A.L. Senkevich, O.M. Borovoy, and A.B. Nadtochii, Doped ZnS:Mn nanoparticles obtained by sonochemical synthesis // *Nano-technology*, **16**, p. 2033 (2005).
13. P.H. Borse, W. Vogel, and S.K. Kulkarni, Effect of pH on photoluminescence enhancement in Pb-doped ZnS nanoparticles // *J. Colloid. Interface Sci.* **293**, p. 437 (2006).
14. S.V. Kozitsky, V.P. Pysarsky, and D.D. Polishchuk, Peculiarities of obtaining of ZnS-polycrystals by means of self-propagating high-temperature synthesis // *PCSS* **4**(4), p. 749 (2003).
15. Yu.V. Vorobiev, S. Jiménez-Sandoval, J. González-Hernández, S.V. Kozitsky, R.V. Zakharchenko, and V.N. Zakharchenko, Electrical and optical properties of semiconducting ZnS and ZnMnS ceramics prepared by self-propagating high-temperature synthesis // *Superficies y Vacio*, **8**, p. 37-41(1999).
16. E.E. Bukke, T.I. Voznesenskaya, N.P. Golubeva, N.A. Gorbacheva, Z.P. Ilyukhina, E.I. Panasik, and M.V. Fok, Separation of complex spectra into individual bands using the generalized method of Alentsev // *Trudy FIAN*, **59**, p. 3-24 (1972), in Russian.
17. L.A. Gromov and V.A. Trofimov // *Zhurnal Fiz. Khim.* **55**(10), p. 2629 (1981), in Russian.
18. G.E. Arhangelskyi, N.N. Grigoriev, and A.V. Lavrov, M.V. Fok, Conversion of the luminescence centers in ZnS-Cu, O at inelastic deformation // *Trudy FIAN*, **164**, p. 103 (1985), in Russian.
19. N.A. Vlasenko, E.N. Pavlova // *J. Opt. Spectrosc.* **12**, p. 550 (1962).
20. Z. P. Ilyukhina, E.P. Panasyuk, V.F. Tunitskaya, and T.F. Filina // *Trudy FIAN*, **59**(38), p. 25-34 (1972), in Russian.
21. M.M. Sychev, E.V. Komarov, L.V. Grigor'ev, S.V. Myakin, I.V. Vasil'eva, A.I. Kuznetsov, and V.P. Usacheva, Gamma and electron beam modification of zinc-sulfide phosphors // *Semiconductors*, **40**, p. 1016 (2006).
22. N.K. Morozova, D.A. Mideros, V.G. Galstian, E.M. Gavrischuk, E.M. Gavrishchuk, Specific features of luminescence spectra of ZnS:O and ZnS:Cu(O) crystals in the context of the theory of nonintersecting bands // *Semiconductors*, **42**(9), p. 1023-1029 (2008).
23. H. Chander, A review on synthesis of nano-phosphors – future luminescent materials // *Proc. ASID'06*, October 8-12, 2006, New Delhi.
24. H. Chander, D. Haranath, K. Jayanthi, and S. Chawla, Structural, optical and photo-luminescence properties of ZnS:Cu nanoparticle thin films as a function of dopant concentration and quantum confinement effect // *Cryst. Res. Technol*. **42**(10), p. 976-982 (2007).
25. J. Zheng, Zh. Zheng, W. Gong, X. Hu, W. Gao, X. Ren, and Haifeng Zhao, Stable, small, and water-soluble Cu-doped ZnS quantum dots prepared via femtosecond laser ablation // *Chem. Phys. Lett.* **465**, p. 275-278 (2008).

26. K. Manzoor, S.R. Vadera, N. Kumar, and T.R.N. Kutty // *Mater. Chem. and Phys.* **82**, p. 718-725 (2003).
27. Ageeth A. Bol, Joke Ferwerda, Jaap A. Bergwerff, Andries Meijerink, Luminescence of nanocrystalline ZnS:Cu^{2+} // *J. Lumin.* **99**, p. 325-334 (2002).
28. F.A. Mir, Structural and optical properties of ZnS nanocrystals embedded in polyacrylamide // *J. Optoelectron. and Biomed. Mater.* **2**(2), p. 79-84 (2010).
29. W.Q. Peng, G.W. Cong, S.C. Qu, and Z.G. Wang, Synthesis and photoluminescence of ZnS:Cu nanoparticles // *Opt. Mater.* **29**, p. 313-317 (2006).
30. J. Pankove, *Optical Processes in Semiconductors.* David Sarnoff Research Center, RCA laboratories; Prentice-Hall Inc. Englewood Cliffs, New Jersey, 1971.
31. Yu.N. Bobrenko, S.Yu. Pavelets, A.M. Pavelets, Effective photoelectric converters of ultraviolet radiation with graded-gap ZnS-based layers // *Semiconductors*, **43**(6), p. 801-806 (2009).